Nanoscopic liquid bridges exposed to a torsional strain

Sophie Sacquin-Mora* and Alain H. Fuchs†
Laboratoire de Chimie Physique, Université de Paris-Sud, F-91405 Orsay Cedex, France

Martin Schoen‡
Stranski-Lab. für Physikalische und Theoretische Chemie, Technische Universität Berlin, Straße des 17. Juni 124, D-10623 Berlin, Germany

(Received 9 July 2003; revised manuscript received 4 September 2003; published 15 December 2003)

In this paper we investigate the response to a torsional strain of a molecularly thin film of spherically symmetric molecules confined to a chemically heterogeneous slit pore by means of Monte Carlo simulations in the grand canonical ensemble. The slit pore comprises two identical plane-parallel solid substrates, the fluid-substrate interaction is purely repulsive except for elliptic regions attracting fluid molecules. Under favorable thermodynamic conditions the confined film consists of fluid bridges where the molecules are preferentially adsorbed by the attractive elliptic regions, and span the gap between the opposite substrate surfaces. By rotating the upper substrate while holding the lower one in position, bridge phases can be exposed to a torsional strain $0 \leqslant \theta \leqslant \pi/2$ and the associated torsional stress T_θ of the (fluidic) bridge phases can be calculated from molecular expressions. The obtained stress curve $T_\theta(\theta)$ is qualitatively similar to the one characteristic of sheared confined films: as the torsion strain increases, T_θ rises to a maximum (yield point) and then decays monotonically to zero. By changing the ellipses' aspect ratio while keeping their area constant, we also investigate the influence of the attractive elliptic patterns' shape on $T_\theta(\theta)$.

DOI: 10.1103/PhysRevE.68.066103 PACS number(s): 62.25.+g, 81.40.Pq, 61.46.+w, 68.55.−a

I. INTRODUCTION

The confinement of a fluid to spaces of nanoscopic dimensions imposes spatial inhomogeneities that have profound consequences on the phase behavior of the fluid [1]. The wealth of new phenomena induced by confinement has been the subject of numerous studies in the last decade, either for simple fluids [2–4] or for more complex cases such as alkane [5] or liquid-crystal films [6]. The behavior of confined fluids becomes even more complex when the confining surfaces are chemically [7,8] or geometrically [9] decorated. For example, one can observe the formation of ''bridge phases'' composed of alternating high(er)and low(er) density portions of fluids. It has now been established that these nanoscopic fluid bridges form as a generic thermodynamic phase in confined systems with structured substrates [10–16].

Molecularly thin films also show a fascinating rheological behavior that is important in many basic and applied problems such as adhesion, lubrication, and friction. It has therefore been under intensive study in recent years, either through theoretical approaches [17–26] or with the help of experimental devices such as the atomic force microscope (AFM) [27–30] or the surface force apparatus (SFA) [31–36]. A particularly interesting phenomenon is the so-called stick-slip motion that has been observed when the confined fluid is exposed to a shear stress. Experimentally the film is sheared by sliding the confining walls over one another. When the walls are separated by only a few molecular diameters, sliding cannot be initiated until a critical stress (the so-called yield stress of the film) is exceeded. The walls then slip over each other, eventually coming to rest, until the critical stress is once again attained, so that this stick-slip cycle repeats itself periodically [37–43].

For reasons well detailed in Ref. [15] almost all the previous theoretical works done on confined fluids have been restricted to high symmetry systems, that is, systems where the fluid properties are translationally invariant in at least one direction parallel to the substrates surfaces. As a consequence of this symmetry condition, one could only study the response of fluid bridges to a shear strain in the direction perpendicular to the direction of the translational invariance [43,44]. Recent works by Sacquin *et al.* showed how one could study the phase behavior of fluids confined in low-symmetry systems using a thermodynamic-integration process [15,16]. In this paper we shall start from the low-symmetry system described in Ref. [15] and be concerned with the response of finite size fluid bridges exposed to a torsional strain. In this study made on fluid bridges under torsion, we shall focus on the comparison of our results with those obtained in shearing experiments, and also on the effect of the fluid bridge's shape when applying the torsional strain.

II. MODEL SYSTEM

The simulation model consists of ''simple'' fluid molecules (i.e., spherically symmetric molecules) confined between the surfaces of two solid substrates. In principle, fluid molecules interact with each other in a pairwise additive fashion via the Lennard-Jones (LJ)(12,6) potential,

$$u(r) = 4\epsilon\left[\left(\frac{\sigma}{r}\right)^{12} - \left(\frac{\sigma}{r}\right)^{6}\right], \tag{1}$$

*Electronic address: sacquin@lcp.u-psud.fr
†Electronic address: alain.fuchs@lcp.u-psud.fr
‡Electronic address: martin@fluids.tu-berlin.de

where ϵ is the well depth, σ the ''diameter'' of a molecule, and r the distance between the centers of a pair of particles. However, for reasons detailed in Ref. [45] we replace $u(r)$ in the subsequent Monte Carlo simulations in the grand canonical ensemble (GCEMC) by

$$u(r)\rightarrow u_{ff}(r) = \begin{cases} u(r)-u(r_c)+du(r)/dr|_{r=r_c}(r_c-r), & r\leqslant r_c \\ 0, & r>r_c, \end{cases} \tag{2}$$

r_c being a cutoff radius whose value will be specified below. From Eq. (2) it is clear that unlike $u(r)$, $u_{ff}(r)$ is explicitly short range.

The confining substrates are both planar, separated by a distance s_z along the z axis of the laboratory coordinate system and semi-infinite, occupying half spaces $-\infty<z\leqslant -s_z/2$ and $s_z/2\leqslant z<\infty$, respectively. They are composed of like atoms interacting with fluid molecules according to the LJ(12,6) potential where the same values of ϵ and σ are employed as for the fluid-fluid interaction. We employ a mean-field approximation for the fluid-substrate potential energy achieved by averaging the (original) fluid-substrate interactions over the positions of the substrate atoms in the x-y plane. This leads to

$$\tilde{\Phi}^{[k]}(z)=\frac{2\pi\epsilon\rho_s\sigma^3}{3}\left[\frac{2}{15}\left(\frac{\sigma}{s_z/2\pm z}\right)^9-\left(\frac{\sigma}{|s_z/2\pm z|}\right)^3\right] =:\varphi^{[k]}_{\rm rep}(z)-\varphi^{[k]}_{\rm att}(z), \tag{3}$$

where the plus and minus signs refer to lower ($k=1$, $z_w=-s_z/2$) and upper ($k=2$, $z_w=+s_z/2$) substrates, respectively, and ρ_s is the (volume) number density of wall atoms. For simplicity we take $\rho_s\sigma^3=1$ throughout this work. Since we treat the substrates as semi-infinite solids, the fluid-substrate attraction is long range, that is, $\varphi^{[k]}_{att}(z)\propto z^{-3}$ [see Eq. (3)].

To model substrate surfaces with imprinted chemical nanopatterns (see Fig. 1) we modify Eq. (3) according to

$$\tilde{\Phi}^{[k]}(z)\rightarrow\Phi^{[k]}(\boldsymbol{r})=\varphi^{[k]}_{\rm rep}(z)-s^{[k]}(x,y;A,B,\kappa)\varphi^{[k]}_{\rm att}(z) =\varphi^{[k]}_{\rm rep}(z)-\phi^{[k]}_{\rm att}(\boldsymbol{r}), \tag{4}$$

where $\boldsymbol{r}$ denotes the (vector) position of a fluid molecule and the ''switching'' function

$$s^{[k]}(x,y;A,B,\kappa)=\frac{1}{1+\exp\left[\kappa\left(\frac{X^{[k]2}}{A^2}+\frac{Y^{[k]2}}{B^2}-1\right)\right]} \tag{5}$$

is introduced as a continuous representation of the Heaviside function (i.e., the Fermi function [46]) such that $\Phi^{[k]}(\boldsymbol{r})$ describes the interaction between a fluid molecule and an infinitesimally smooth, repulsive solid surface decorated with an attractive elliptical area of (fixed) semiaxis A and B (and infinite height in the $\pm z$ directions) centered at (0,0, $\pm s_z/2$). In Eq. (5), $\kappa\geqslant 0$ is a measure of the ''softness'' with which the attractive part of $\Phi^{[k]}(\boldsymbol{r})$ is turned off as a fluid molecule moves away from the center of the elliptical area, that is from the point (0,0) in the x-y plane (see Fig. 2 in Ref. [15]). We also have

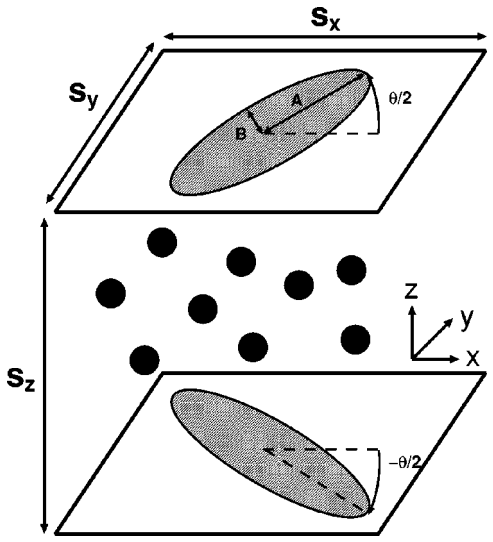

FIG. 1. A schematic diagram of a simple fluid (black circles) confined by two chemically decorated substrates. Outside of the elliptic attractive regions (in gray) the fluid-substrate interaction is purely repulsive.

$$X^{[1]}=x\cos(-\theta/2)+y\sin(-\theta/2),$$
$$Y^{[1]}=y\cos(-\theta/2)-x\sin(-\theta/2), \tag{6}$$

for the lower substrate and

$$X^{[2]}=x\cos(\theta/2)+y\sin(\theta/2),$$
$$Y^{[2]}=y\cos(\theta/2)-x\sin(\theta/2), \tag{7}$$

for the upper one, in order to model the angle θ between the large axis of the two ellipses (see Fig. 1).

III. THERMOMECHANICAL PROPERTIES

A. Thermodynamic considerations

From a thermodynamic perspective we refer to the ''system'' as a finite lamella of the confined (infinite in the x and y directions) fluid having dimensions $s_x\times s_y\times s_z$. The remainder of the film and the walls constitute the environment. The lamella can exchange compressional work with the environment by altering s_z or by changing the distance between the imaginary planes located at $x/s_x=\pm 0.5$ and $y/s_y=\pm 0.5$, which act like virtual ''pistons.'' In addition, the system can be exposed to a torsional strain θ [see Eqs. (6) and (7)]. The mechanical work due to infinitesimal compressional and torsional strains can be expressed as

$$dW=\sum_\alpha A_\alpha T_{\alpha\alpha}ds_\alpha+VT_\theta d\theta, \tag{8}$$

where $V=s_x s_y s_z$ is the volume of the lamella, A_α the area of the α directed face of the lamella, and $T_{\alpha\alpha}$ ($\alpha=x,y,z$) are diagonal elements of the stress tensor **T**. The absence of off-diagonal elements of **T** signifies that we ignore work due to shear forces in this study. In Eq. (8) we also introduce the torsional stress T_θ conjugate to the torsional strain θ. In addition, the lamella is materially and thermally coupled to its environment, that is, thermodynamically it constitutes an open system. Hence, reversible transformations of the lamella are governed by the grand potential whose exact differential is given by

$$d\Omega(T,\mu,V,\theta)=-\mathcal{S}dT-Nd\mu+dW. \tag{9}$$

In Eq. (9), $\mathcal{S}$ denotes entropy, T represents temperature, and N is the number of fluid molecules.

The link between the macroscopic and molecular scales is the well-known statistical thermodynamic relation [46]

$$\Omega=-\beta^{-1}\ln\Xi=-\beta^{-1}\ln\sum_{N=0}^{\infty}\frac{\exp(\beta\mu N)}{\Lambda^{3N}N!}Z, \tag{10}$$

where $\beta=1/k_BT$ (k_B Boltzmann's constant), Λ is the thermal de Broglie wavelength and the far right side obtains after the usual integration over momentum subspace. The configuration integral is given by

$$Z=\int_{V^N}d\boldsymbol{r}\,\exp[-\beta U(\boldsymbol{r}^N)]. \tag{11}$$

In Eq. (11), $\boldsymbol{r}^N:=\{\boldsymbol{r}_1,\boldsymbol{r}_2,\ldots,\boldsymbol{r}_N\}$ denotes a particular configuration of N fluid molecules and

$$U(\boldsymbol{r}^N)=\frac{1}{2}\sum_{i=1}^{N}\sum_{j=1\neq i}^{N}u_{ff}(r_{ij})+\sum_{k=1}^{2}\sum_{i=1}^{N}[\varphi_{\mathrm{rep}}^{[k]}(z_i)-s^{[k]}(x,y;A,B,\kappa)\varphi_{\mathrm{att}}^{[k]}(z_i)]=U_{FF}+U_{FS} \tag{12}$$

is the configurational energy.

B. Molecular expression for the torsional stress

From Eq. (9) we have the purely thermodynamic expression

$$VT_\theta=\left(\frac{\partial\Omega}{\partial\theta}\right)_{T,\mu,V}. \tag{13}$$

Combining Eq. (13) with the statistical expressions given in Eqs. (10)–(12), we obtain

$$T_\theta=-(V\beta\Xi)^{-1}\sum_{N=0}^{\infty}\frac{\exp(\beta\mu N)}{\Lambda^{3N}N!}\left(\frac{\partial Z}{\partial\theta}\right)_{T,V}=-(V\Xi)^{-1}\sum_{N=0}^{\infty}\frac{\exp(\beta\mu N)}{\Lambda^{3N}N!}\int_{V^N}d\boldsymbol{r}\,\exp[-\beta U(\boldsymbol{r}^N)]\times\left(\frac{\partial U_{FS}}{\partial\theta}\right)_{T,V}. \tag{14}$$

Since the switching function s is the only part of the configurational energy that depends on θ, we eventually have

$$T_\theta=\frac{1}{V}\left\langle\sum_{k=1}^{2}\sum_{i=1}^{N}-\left(\frac{\partial s^{[k]}(x_i,y_i)}{\partial\theta}\right)\varphi_{att}^{[k]}(z_i)\right\rangle=-\frac{1}{V}\left\langle\sum_{k=1}^{2}F_\theta^{[k]}\right\rangle. \tag{15}$$

We can notice that since $\Omega(\theta)=\Omega(-\theta)$, i.e., the grand potential is an even function of the torsion strain, the torsion stress T_θ is an odd function of θ.

Another quantity of interest in the context of this work is the torsion modulus

$$\mu_\theta=\frac{1}{V}\left(\frac{\partial^2\Omega}{\partial\theta^2}\right)_{T,\mu,V}=\frac{1}{V}\left(\frac{\partial T_\theta}{\partial\theta}\right)_{T,\mu,V}, \tag{16}$$

which is the equivalent in torsion to the shear modulus c_{44} [47] used in studies done on the shearing of confined fluids. By a calculation parallel to the one detailed in Ref. [42] one can show from Eqs. (10)–(15) and (16) that

$$\mu_\theta=\frac{1}{V}\left\langle\frac{\partial^2U_{FS}}{\partial\theta^2}\right\rangle-\frac{\beta}{V}[\langle(F_\theta^{[1]}+F_\theta^{[2]})^2\rangle-\langle F_\theta^{[1]}+F_\theta^{[2]}\rangle^2]. \tag{17}$$

From Eqs. (15) and (17) it is also clear that

$$\frac{\partial^2U_{FS}}{\partial\theta^2}=\frac{\partial F_\theta^{[1]}}{\partial\theta}+\frac{\partial F_\theta^{[2]}}{\partial\theta}. \tag{18}$$

C. Technical aspects

We carried out GCEMC where the chemical potential μ, temperature T, volume V, and torsional strain θ are fixed. As explained in detail in Ref. [45], the generation of a Markov chain of $m=1,\ldots,M$ configurations $\{\boldsymbol{r}_m^N\}$ in GCEMC proceeds in pairs of events: trial displacements and attempts to create or destroy fluid molecules. Both events are realized according to the probability density governing the grand canonical ensemble. If a particular configuration k contains N_k fluid molecules, the sequence of N_k displacements followed by N_k creation-destruction attempts constitutes a "GCEMC cycle." Results presented below are based upon runs of 10^6–10^7 MC cycles with $N\simeq 300$. In all the simulations we set $r_c=2.5$ [see Eq. (2)].

In what follows all quantities will be given in the customary dimensionless (i.e., "reduced") units: length is expressed in units of σ, energy in units of ϵ, and temperature in units of ϵ/k_B; other quantities are expressed in terms of suitable combination of these "basic" quantities. We employ standard periodic boundary conditions at the planes $x=\pm s_x/2$, $y=\pm s_y/2$ where $s_x=s_y=30$. These latter values are large enough (if A and B are small enough) to mimic an infinitely large system with a *single* isolated attractive elliptic region per substrate. Hence, in the actual simulations we associate the computational cell with the fluid lamella introduced in

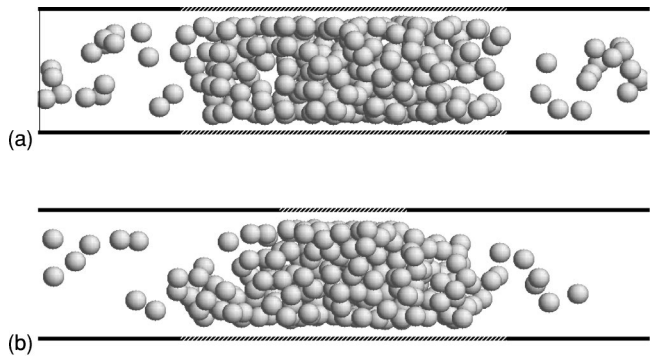

FIG. 2. Snapshots of two representative configurations of the system for $T=0.70$, $\mu=-8.00$, $s_z=6.0$, $A=8$, and $B=3.125$. (a) $\theta=0$, (b) $\theta=\pi/2$.

Sec. III A. We have for the ''switching parameter'' $\kappa=125$, which causes $s(x,y;A,B,\kappa)$ to vary between zero (i.e., no fluid-substrate attraction) and one (i.e., full fluid-substrate interaction) [see Eqs. (4) and (5)] over an elliptical shell of thickness $\Delta r \simeq 0.2$.

IV. RESULTS

Our results were obtained for $T=0.70$ and $\mu=-8.0$. Under the present thermodynamic conditions, and for $0 \leqslant \theta \leqslant \pi/2$ (the torsion angle value is limited by the symmetry of the system), the confined fluid forms a ''bridge'' phase; that is, a high(er)-density portion of the fluid is stabilized between the adsorbing elliptic patterns on the substrates, whereas a low(er)-density regime exists over their repulsive outer part. This characteristic structure is illustrated by the snapshots of two representative configurations for $\theta=0$ and $\theta=\pi/2$ in Fig. 2, and by the contour plots of the local density $\rho(x,y,z)$ in Figs. 3 and 4. The plots in Fig. 3(a) and 3(b) show sequences of ''islands'' along the z axis surrounded by a closed line of lower density. The islands are well resolved and separated by a distance of approximately $\Delta z \simeq 1$ between centers of neighboring islands. They indicate stratification of the fluid in the direction perpendicular to the substrates (i.e., along the z axis). In the symmetric case $\theta=0$, the high-density islands have roughly the same size in transverse directions (i.e., x or y) [see Figs. 3(a) and 3(b)]; while for $\theta=\pi/2$, their shape changes as z goes from -3 to 3 [see Figs. 4(a) and 4(b)], thus reflecting the rotation of the attractive elliptic patterns on the substrates ($|z|=3$).

Bridge phases may coexist with liquidlike or gaslike phases characterized by high(er)- and low(er)-density fluids, respectively, occupying the entire volume of the system (similar to Fig. 4(a) and 4(c) in Ref. [15])

A. Torsion curves: general features

The key quantity calculated in the present Monte Carlo simulations is the torsional stress $T_\theta(\theta)$ accessible via the Eqs. (13)–(15). A typical torsion curve is shown in Fig. 5;

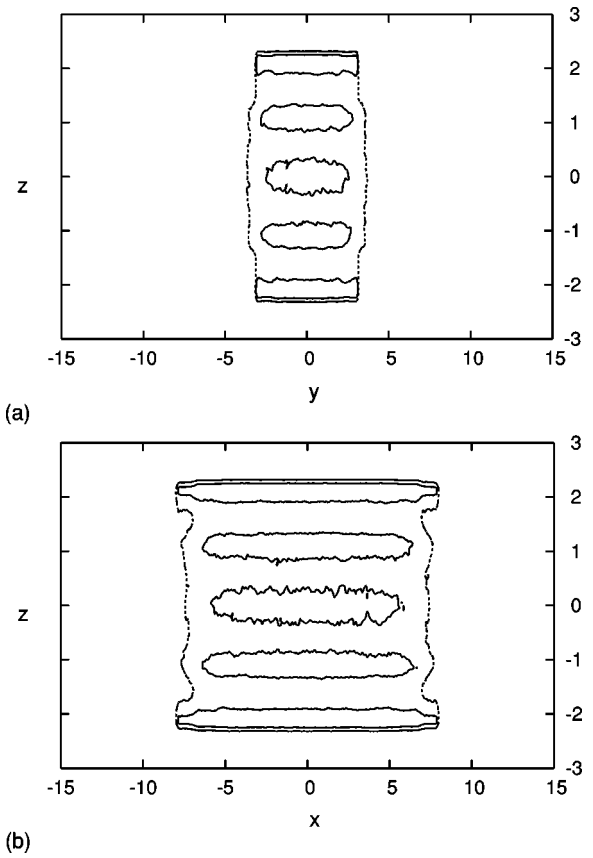

FIG. 3. Contour lines $\rho=0.25$ (-), 0.75 (–) for $T=0.70$, $\mu=-8.00$, $s_z=6.0$, $A=8$, $B=3.125$, and $\theta=0$. (a) $\rho(y,z)$ in the $x=0$ plane, (b) $\rho(x,z)$ in the $y=0$ plane.

regardless of the thermodynamic state and the shape [i.e., A and B, see Eq. (5)] of the elliptic pattern, it exhibits the following features.

(1) For vanishing torsional strain (i.e., $\theta=0$), $T_\theta \equiv 0$ for symmetry reasons.

(2) If exposed to a sufficiently small torsional strain θ, $T_\theta(\theta)$ depends linearly on θ according to Hooke's law.

(3) As the torsional strain increases, the bridge responds increasingly nonlinearly so that the torsional stress reaches a maximum, declines, and eventually vanishes. The maximum of the torsion stress curve determines a yield point $(\theta^{yd}, T_\theta^{yd})$.

(4) For symmetry reasons we also have $T_\theta(\pi/2) \equiv 0$.

These general characteristics have also been observed previously in the case of stress curves for simple fluid films confined between planar-parallel substrates, when these films were exposed to a shear strain. In these latter calculations the confining substrates were either chemically homogeneous but atomically structured (i.e., discrete) [42,17,37,22,41,24] or decorated with alternating striplike domains composed of different solid materials [43,44]. As θ departs from 0 the fluid bridge becomes less elastic, eventually deforming plastically, until T_θ reaches a maximum where the torsion modulus μ_θ vanishes [see Eq. (16)]. T_θ^{yd} is the maximum torsion stress the fluid bridge can sustain when rotating one substrate

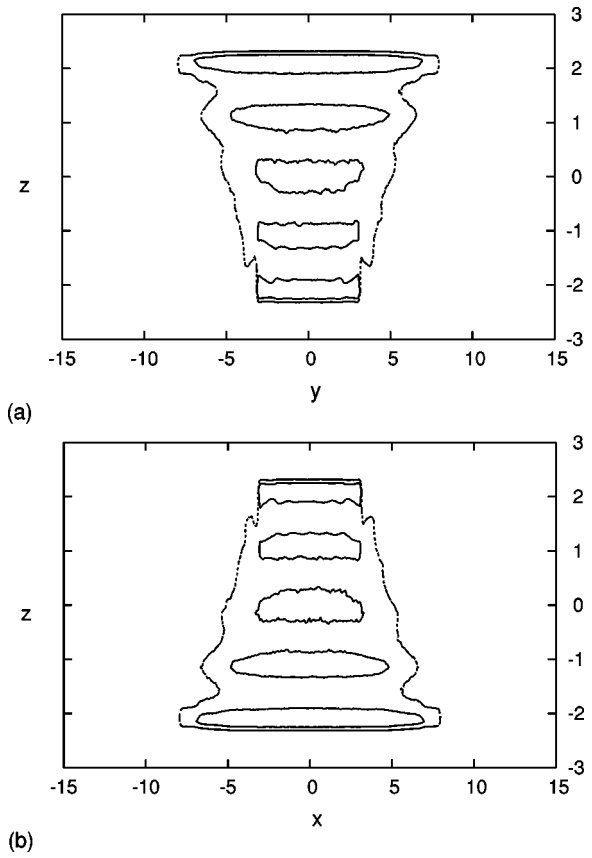

FIG. 4. Contour lines $\rho=0.25$ (-), 0.75 (–) for $T=0.70$, $\mu=-8.00$, $s_z=6.0$, $A=8$, $B=3.125$, and $\theta=\pi/2$. (a) $\rho(y,z)$ in the $X^{[1]}=0$ plane, (b) $\rho(x,z)$ in the $Y^{[1]}=0$ plane [see Eq. (6) for the definitions of $X^{[1]}$ and $Y^{[1]}$].

over the other while the thermodynamic state variables (μ, T, and s_z) are held fixed. These results lead us to think there should also exist for fluids exposed to a torsional strain a rotating and a sticking regime that are separated by the yield point (θ^{yd},T_θ^{yd}), and similar to the sticking and slipping regimes encountered for sheared confined fluids. Thermodynamic states for $\theta \leqslant \theta^{yd}$ are mechanically stable so that the walls ''stick'' to the fluid film. When $\theta \geqslant \theta^{yd}$ these states become mechanically unstable and the walls can ''rotate'' freely over the surface of the film (see Ref. [42]). From the definition of the torsion modulus in Eq. (16) and the fact that the yield point represents a maximum of the torsion stress curve it also follows that $\mu_\theta > 0$ in the sticking regime and that $\mu_\theta < 0$ in the rotating regime.

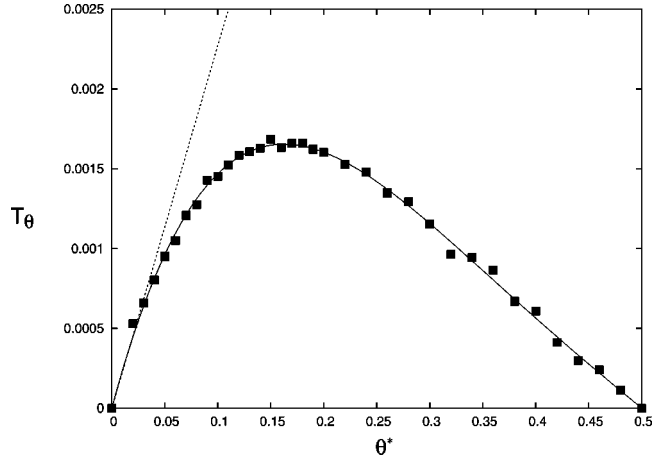

FIG. 5. A typical torsion stress curve $T_\theta(\theta^*)$ (where $\theta^*=\theta/\pi$) for $A=8$ and $C=3.125$. The solid line is intended to guide the eye and the dotted line corresponds to the Hookean limit.

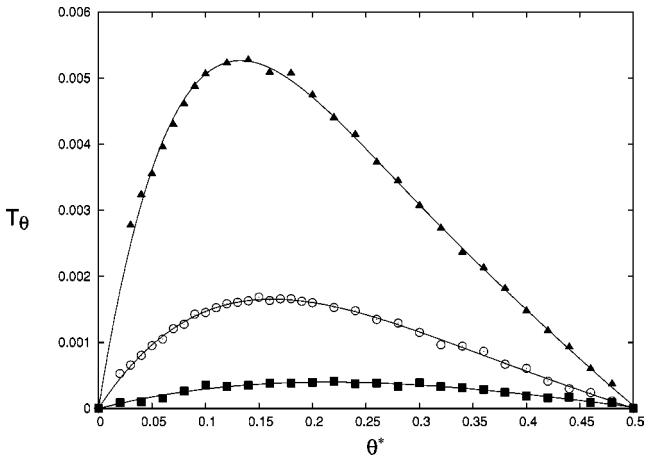

FIG. 6. Torsion stress $T_\theta(\theta^*)$ for $A=8$, $B=3.125$, and $s_z=4.0$ (▲), $s_z=6.0$ (○), $s_z=10.0$ (■). Solid lines are intended only to guide the eye.

Because of the linear dependance in θ of T_θ at small deformations, the slope of the torsion curve for $\theta=0$ gives us $\mu_\theta(0)$. It provides an information on the stiffness of the fluid bridge at rest (i.e., when $\theta=0$), that is, its ability to sustain a torsional strain. In Fig. 5 the torsion modulus $\mu_\theta(0)$ computed from the expression in Eq. (17) has been used to determine the tangent to the shear stress curve at $\theta=0$, which also illustrates the reliability of our calculations.

Furthermore, for larger substrates separations, we observe a decrease of the torsional yield stress T_θ^{yd} and an increase of the yield strain θ^{yd} (see Fig. 6). This behavior is again qualitatively similar to the one observed earlier for confined fluids exposed to a shear strain (see Refs. [17,41] and Fig. 6(a) in Ref. [43]). It can be rationalized by an argument similar to the one given in Ref. [41]: as the number of layers in the bridge increases, the structure of the central layers becomes less ordered (even though the elliptic bridges do not show any crystalline structure), and it takes less force to wring the fluid bridge.

However in Ref. [43] the yield stress obtained by shearing monolayer up to trilayer bridges scales approximately with the inverse wall separation, while in our case we observe a much faster decay of the maximum torsional stress with s_z^{-3}. If the bridges were solidlike their torsional stiffness would scale linearly with their cross-sectional area and inversely with their length, the reason being that the area is a measure for how many (metaphoric) springs act ''in parallel'' holding the particles together, while the length of the bridge indicates how many springs act ''in series.'' Therefore when we increase the size of a solid bridge, while maintaining its shape, its effective torsional stiffness will grow. However,

here we observe a decrease of the torsional yield stress with $1/s_z^3$, which means that the torsional stiffness of the bridge becomes weaker with increasing the system size even if we assume proportionality with the area of contact, thus emphasizing the nonsolid character of the bridges formed under the present conditions.

We also note that the values of the torsional stress sustained by the elliptic bridges are much smaller (one to two orders of magnitude) compared with the shear stress values supported by fluid bridges as reported in Ref. [43]. Still, a more quantitative comparison does not make too much sense at this point since both the systems studied in the earlier shear work and the observables differ from those considered here. The lower value of T_θ^{yd} and its faster decay with the wall separation can be explained qualitatively as follows: The deformation of fluid by shearing leads to a perturbation of the fluid bridge's structure in only one dimension, namely, in the direction in which the shear strain is applied. On the other hand, the torsion of fluid bridges induces a two-dimensional displacement of the particles in the fluid bridge (that is, along the two lateral directions x and y), so that the associated perturbation of its structure is much more pronounced in this case than for sheared bridges. As a consequence the ability of fluid bridges to resist torsional deformations is greatly reduced in comparison with their ability to resist shear deformation, as long as the shear strain is applied only in one dimension as in all the previous studies.

B. The impact of the ellipses shape

In our model shape and size of the attractive elliptic chemical pattern decorating the substrates turns out to have significant consequences for the yield-point location $(\theta^{yd}, T_\theta^{yd})$. As we already mentioned in Sec. IV A, earlier works on fluid bridges showed that the area of the attractive chemical patterns has to be large enough for bridge morphologies to be thermodynamically stable. In this work we fixed the area of the ellipses to $AB\pi = 25\pi$ and looked at the torsion curves for different values of the large semiaxis A (see Fig. 7). For the subsequent discussion it is convenient to introduce the aspect ratio $r_a = A/B > 1$ of the ellipses.

Once again we can check the good agreement between the values of $\mu_\theta(0)$ obtained from Eq. (17) and the slope of the shear stress curve at $\theta = 0$ (see the dotted lines in Fig. 7). More significantly, this time they also reveal substantial deviations from Hookean behavior at very small torsional strains. For example, the plastic regime begins already at $\theta/\pi \gtrsim 0.05$ when $r_a \gtrsim 2$ [see Figs. 5 and 7(c)–(e)]. As we move away from the perfectly symmetric case $r_a = 1$, where the chemical patterns degenerate to circles, the deviation from the elastic linear behavior while increasing θ occurs earlier.

For fixed $s_z = 6.0$ one can see from Table I that θ^{yd} decreases while T_θ^{yd} increases monotonically with increasing aspect ratio. We observe an evolution from "soft" bridges with low T_θ^{yd} and larger θ^{yd} to more "rigid" ones where T_θ^{yd} is larger but θ^{yd} is smaller. This "rigidity" is also reflected by the increase of $\mu_\theta(0)$ with r_a (see Table I).

We also tried to renormalize the stress curves plotted in Fig. 8 in order to know whether or not the results obtained by Bock and Schoen in Ref. [43] concerning the universality of the shear stress curves could also be applied to twisted fluid bridges. However our renormalized data failed to fall on an unique curve or to coincide with the universal curve obtained in Ref. [43], thus pointing out another difference between the responses to shear and torsional deformations of fluid bridges. The increased perturbation of the bridge's structure that we pointed out in Sec. IV A precludes the use of a small-strain approximation to describe the torsional curves in the range $0 \leqslant \theta \leqslant \theta^{yd}$ similar to the one suggested by Bock and Schoen [43].

V. DISCUSSION AND CONCLUSIONS

In this paper we employ GCEMC simulations to investigate the rheological properties of a fluid confined between nanopatterned substrates of low symmetry. The interaction between fluid molecules and the planar substrates is purely repulsive, i.e., the solid is not wetted by the fluid. However, each substrate is decorated with an elliptic chemical pattern that adsorbs fluid molecules preferentially. Under favorable thermodynamic conditions a higher-density portion of the confined fluid stabilized by the attractive chemical patterns is surrounded by a lower-density portion supported by the repulsive parts of the substrates, thus forming what we call a bridge phase. By rotating the elliptic patterns in opposite directions, these bridge phases can be exposed to a torsional strain θ and the associated torsional stress T_θ can be calculated from molecular expressions.

As we can see in all our plots of $T_\theta(\theta)$, the elliptic bridges can sustain a nonvanishing torsional strain, even though they have a noncrystalline structure. This property is a direct consequence of the lack of cylindrical symmetry of the system and can be compared to the way the fluid bridges in Ref. [43] show a resistance to *shear* deformations because of their inhomogeneity in the direction of the applied shear stress. Furthermore, the torsion curves obtained for twisted fluid bridges are *qualitatively* similar to those obtained for confined sheared fluids (being solidlike or not) in that they exhibit a Hookean regime for small torsional strains and a yield point on account of an increasingly plastic response at higher angles (see Fig. 5). Yet when we begin to deform fluid bridges, the plastic regime appears much earlier in the case of torsion than for shearing. The evolution of the yield torsional stress when increasing the substrates' separation is also the same for twisted and sheared fluids. In both cases we observe a decrease of T_θ (see Fig. 6), but the decay of the yield stress is much faster in the case of torsion (where T_θ^{yd} scales approximately with $1/s_z^3$). It also turns out that the values of torsional stresses we obtained during this study were always much smaller than any shear stress values obtained in previous works. These two properties can be connected to the fact that torsional deformations induce a much greater perturbation in the bridge's inner structure than shear deformations.

When modifying the ellipses shape, i.e., their aspect ratio r_a, the evolution in the yield point permits us to distinguish

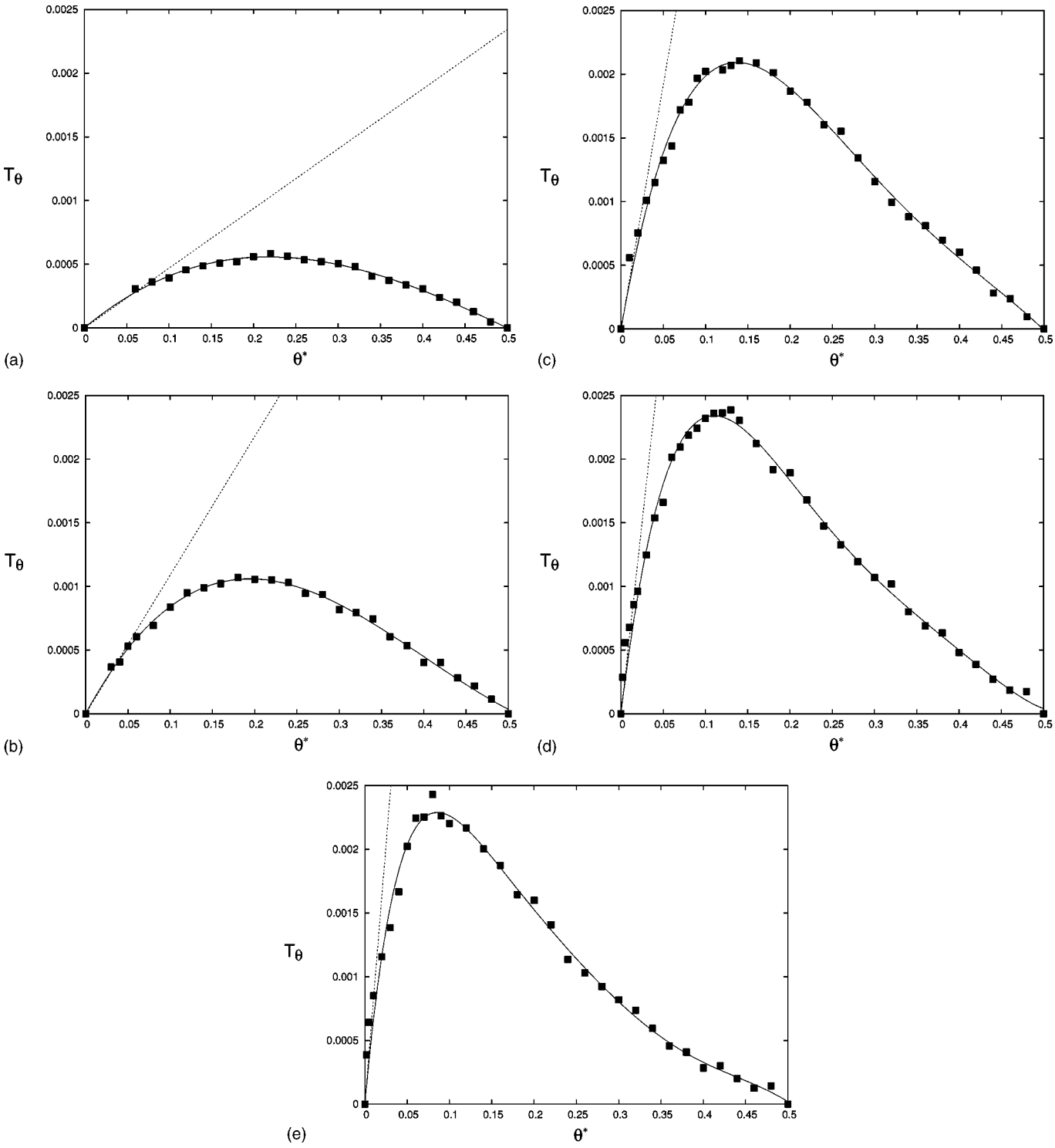

FIG. 7. Torsion stress curves $T_\theta(\theta^*)$ for $s_z=6.0$, $AB=25$, and different aspect ratios. (a) $r_a=1.5625$, (b) $r_a=1.9600$, (c) $r_a=3.2400$, (d) $r_a=4.0000$, and (e) $r_a=5.0625$. The solid line is intended to guide the eye while the dotted one corresponds to the Hookean limit.

between soft and rigid bridges. As r_a increases we have a continuous change from soft bridges, which are easily distorted (high θ^{yd} and low T_θ^{yd}), to more rigid ones (low θ^{yd} and high T_θ^{yd}). The renormalization of the different torsion curves obtained when changing r_a within the theory of corresponding states [46] fails to give satisfying results, which is another consequence of the increased sensitivity of fluid bridges to torsional deformation compared to shearing.

Many possibilities now appear for future investigations of fluid bridges under torsion. First, we intend to work further on the stick-rotate transition and develop a more adequate ensemble with a fixed torsional stress T_θ where the torsional

TABLE I. Evolution of the yield point's coordinates $(\theta^{yd}, T_\theta^{yd})$ and of the torsion modulus at rest $\mu_\theta(0)$ [see Eq. (17)] when modifying the aspect ratio r_a of elliptic patterns with a constant area $AB\pi = 25\pi$.

r_a	θ^{yd}	T_θ^{yd}	$\mu_\theta(0)$
1.5625	0.22π	5.8448×10^{-4}	4.6869×10^{-3}
1.9600	0.18π	1.0687×10^{-3}	1.08853×10^{-2}
2.5600	0.15π	1.6861×10^{-3}	2.2708×10^{-2}
3.2400	0.14π	2.1054×10^{-3}	3.8351×10^{-2}
4.0000	0.13π	2.3864×10^{-3}	6.0061×10^{-2}
5.0625	0.08π	2.4304×10^{-3}	8.1377×10^{-2}

strain θ can fluctuate, similar to the grand isostress ensemble introduced by Bordarier *et al.* [42]. Another subject of interest will be the phase behavior of a fluid between low-symmetry substrates. Using the thermodynamic integration method for computing the grand potential Ω in such systems that has already been developed in Ref. [15], different studies on the combined effects of torsion and chemical potential [12,13] can be made. Eventually, a last but very interesting direction will be to develop an analysis of phase transitions induced by the torsion of fluid bridges with an approach similar to what has been done in Ref. [48], that is, using Landau's phenomenological theory of phase transitions and the torsion modulus μ_θ as an order parameter.

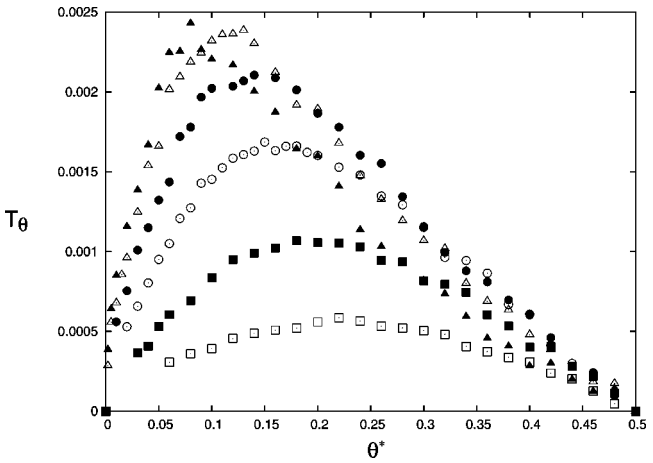

FIG. 8. Torsion stress curves as in Fig. 6 but on the same scale. (□) $r_a = 1.5625$, (■) $r_a = 1.9600$, (○) $r_a = 2.5600$, (●) $r_a = 3.2400$, (△) $r_a = 4.0000$, and (▲) $r_a = 5.0625$.

ACKNOWLEDGMENT

M.S. is grateful for support from the Sonderforschungbereich 448 ''Mesoskopische strukturierte Verbundsysteme.''

[1] S. Dietrich, J. Phys.: Condens. Matter **10**, 11469 (1998).
[2] H.K. Christenson, Colloids Surf., A **123-124**, 355 (1997).
[3] A.G. Salinger and L.J. Douglas Frink, J. Chem. Phys. **118**, 7457 (2003).
[4] L.J. Douglas Frink and A.G. Salinger, J. Chem. Phys. **118**, 7466 (2003).
[5] F. Porcheron, B. Rousseau, and A.H. Fuchs, Mol. Phys. **100**, 2109 (2002).
[6] T. Gruhn and M. Schoen, Phys. Rev. E **55**, 2861 (1997).
[7] M. Schoen and D.J. Diestler, Phys. Rev. E **56**, 4427 (1997).
[8] M. Schoen and D.J. Diestler, Chem. Phys. Lett. **270**, 339 (1997).
[9] M. Schoen and S. Dietrich, Phys. Rev. E **56**, 499 (1997).
[10] P. Röcken, A. Somoza, P. Tarazona, and G.H. Findenegg, J. Chem. Phys. **108**, 8689 (1998).
[11] H. Bock and M. Schoen, Phys. Rev. E **59**, 4122 (1999).
[12] H. Bock and M. Schoen, J. Phys.: Condens. Matter **12**, 1569 (2000).
[13] H. Bock, D.J. Diestler, and M. Schoen, J. Phys.: Condens. Matter **13**, 4697 (2001).
[14] M. Schoen, Colloids Surf., A **206**, 253 (2002).
[15] S. Sacquin, M. Schoen, and A.H. Fuchs, Mol. Phys. **100**, 2971 (2002).
[16] S. Sacquin, M. Schoen, and A.H. Fuchs, J. Chem. Phys. **118**, 1453 (2003).
[17] M. Schoen, C.L. Rhykerd, Jr., D.J. Diestler, and J.H. Cushman, Science **245**, 1223 (1989).
[18] P.A. Thompson and M.O. Robbins, Phys. Rev. A **41**, 6830 (1990).
[19] P.A. Thompson, G.S. Grest, and M.O. Robbins, Phys. Rev. Lett. **68**, 3448 (1992).
[20] M. Lupkowski and F. van Swol, J. Chem. Phys. **95**, 1995 (1991).
[21] G.H. Peters and D.J. Tildesley, Phys. Rev. E **52**, 1882 (1995).
[22] M. Schoen, D.J. Diestler, and J.H. Cushman, J. Chem. Phys. **100**, 7707 (1994).
[23] G.H. Peters and D.J. Tildesley, Phys. Rev. E **54**, 5493 (1996).
[24] P. Bordarier, B. Rousseau, and A.H. Fuchs, Thin Solid Films **330**, 21 (1998).
[25] R. Khare, J. de Pablo, and A. Yethiraj, J. Chem. Phys. **114**, 7593 (2001).
[26] A.E. Filippov, J. Klafter, and M. Urbakh, Phys. Rev. Lett. **87**, 275506 (2001).
[27] C.M. Mate, G.M. McClelland, R. Erlandsson, and S. Chiang, Phys. Rev. Lett. **59**, 1942 (1987).
[28] S. Fujisawa, E. Kishi, Y. Sugawara, and S. Morita, Phys. Rev. B **51**, 7849 (1995).
[29] H. Hölscher, U.D. Schwarz, O. Zwörner, and R. Wiesendanger, Phys. Rev. B **57**, 2477 (1998).
[30] R. Bennewitz, T. Gyalog, M. Guggisberg, M. Bammerlin, E. Meyer, and H.-J. Güntherodt, Phys. Rev. B **60**, R11301 (1999).
[31] J.N. Israelachvili, *Intermolecular and Surface Forces* (Academic, London, 1992).
[32] J.N. Israelachvili, P.M. McGuiggan, and A.M. Homola, Science **240**, 189 (1988).
[33] J.N. Israelachvili and P.M. McGuiggan, Science **241**, 795 (1988).

[34] S. Granick, Science **253**, 1374 (1991).
[35] H.-W. Hu, G.A. Carson, and S. Granick, Phys. Rev. Lett. **66**, 2758 (1991).
[36] C. Drummond and J. Israelachvili, Phys. Rev. E **63**, 041506 (2001).
[37] M. Schoen, D.J. Diestler, and J.H. Cushman, Phys. Rev. B **47**, 5603 (1993).
[38] M.L. Gee, P.M. McGuiggan, and J.N. Israelachvili, J. Chem. Phys. **93**, 1895 (1990).
[39] J. Klein and E. Kumacheva, J. Chem. Phys. **108**, 6996 (1998).
[40] E. Kumacheva and J. Klein, J. Chem. Phys. **108**, 7010 (1998).
[41] M. Schoen, S. Hess, and D.J. Diestler, Phys. Rev. E **52**, 2587 (1995).
[42] P. Bordarier, M. Schoen, and A.H. Fuchs, Phys. Rev. E **57**, 1621 (1998).
[43] H. Bock and M. Schoen, J. Phys.: Condens. Matter **12**, 1545 (2000).
[44] H. Bock, D.J. Diestler, and M. Schoen, Phys. Rev. E **64**, 046124 (2001).
[45] D.J. Diestler and M. Schoen, Phys. Rev. E **62**, 6615 (2000).
[46] D.A. McQuarrie, *Statistical Mechanics* (Harper & Row, New York, 1976), Chap. 10-2.
[47] H.B. Callen, *Thermodynamics* (Wiley, New York, 1960), Chap. 13.
[48] V.L. Popov, Solid State Commun. **115**, 369 (2000).